

BRIEF REPORT

srGAP2 deactivates RhoA to control the duration of thrombin-mediated endothelial permeability

Alba Lopez Rioja, Ashton Faulkner and Harry Mellor 

School of Biochemistry, Biomedical Sciences Building, University of Bristol, Bristol, UK

Correspondence should be addressed to H Mellor: h.mellor@bristol.ac.uk

Abstract

The endothelial barrier is a tightly regulated gateway in the transport of material between circulation and the tissues. Inflammatory mediators such as thrombin are able to open paracellular spaces in the endothelial monolayer to allow the extravasation of plasma proteins and leukocytes. Here we show that the protein SLIT-ROBO Rho GTPase-activating protein 2 (srGAP2) plays a critical role in regulating the extent of thrombin-mediated opening. We show that srGAP2 is not required for normal barrier function in resting endothelial cells, but that depletion of srGAP2 significantly increases the magnitude and duration of junctional opening in response to thrombin. We show that srGAP2 acts to switch off RhoA signaling after the contraction phase of thrombin-induced permeability, allowing respreading of cells and reformation of the barrier. srGAP2 is also required for effective restoration of the barrier after treatment with two other vasoactive agents that activate RhoA – TNF α and angiotensin II. Taken together, we show that srGAP2 has a general function in controlling RhoA signaling in endothelial permeability, acting to limit the degree and duration of opening, by triggering the switch from endothelial cell contraction to respreading.

Key Words

- ▶ actin cytoskeleton
- ▶ endothelial
- ▶ permeability
- ▶ RhoA
- ▶ srGAP2

Introduction

Endothelial cells (ECs) line the inner surface of blood and lymph vessels, forming an active barrier between the circulation and the underlying tissue (1). This barrier must be tightly regulated to control the exchange of metabolites, proteins and leukocytes between the two compartments. Material can cross the endothelial barrier via both transcellular and paracellular routes (2). For transcellular transport, ECs deploy a diverse set of channels, transporters, pores and vesicular trafficking pathways in order to move molecules across the body of the cell (3).

The paracellular route is simpler in that it requires only the opening of the junctions between ECs to allow

material to exchange. The consequences of opening gaps in the endothelial barrier, however, means that the process must be tightly controlled. ECs are connected to each other by adherens junctions and tight junctions to form a barrier that excludes all but small molecules (4). The organization of these junctions varies throughout the circulation, from the highly organized and impermeable blood–brain barrier to the loosely organized junctions of lymphatic ECs. Triggering local paracellular permeability is important in inflammation and infection, where leukocytes have to leave the vessels to resolve the issue (5), and local barrier function is regulated acutely by a host of vasoactive agents.

Opening the EC junctions requires disassembly of cell-cell junctions and contraction of the actin cytoskeleton to open a gap between the cells (6). Junctional complexes are linked mechanically to the actin cytoskeleton and as junctions are dismantled, cells exert contractile force on this interface causing the opening of a paracellular gap. Re-establishment of barrier function requires a switch from cell contraction to cell respreading, and reassembly of the cell-cell junction complexes (7). The Rho GTPase family of signaling proteins are the master regulators of the actin cytoskeleton and also regulate the assembly of cell-cell junctions – positioning them to regulate and coordinate these processes (8).

Despite the key roles of Rho GTPases in regulating endothelial permeability, we still know little of how they themselves are regulated in this process. Canonical members of the family such as RhoA, Rac1 and Cdc42 are switched on by Rho guanine nucleotide exchange factors (GEFs; (9)) and switched off by Rho GTPase accelerating proteins (GAPs; (10)). Both are large families of signaling proteins, with multi-domain structures that allow them to make distinct interactions and target distinct cellular locations. In recently published work, Amado-Azevedo and colleagues performed a screen of over 270 Rho GTPase-associated genes to identify novel signaling proteins in the regulation of endothelial permeability by thrombin. As part of that work, they identified SLIT-ROBO Rho GTPase-activating protein 2 (srGAP2), a poorly characterized member of the Rho GAP family, and showed that it was important for the recovery of barrier integrity after thrombin treatment (11). Here we investigate the mechanism of srGAP2 action and show that srGAP2 is required for the termination of RhoA signaling after thrombin treatment. Depletion of srGAP2 had no effect on resting barrier function, but significantly increased permeability in thrombin-treated cells and delayed recovery of barrier function. Importantly, srGAP2 was also required for recovery from other vasoactive mediators that target RhoA, suggesting that it plays a fundamental role in the RhoA-mediated regulation of the endothelial barrier.

Materials and methods

Materials

Human angiotensin II (Ang II) was from Sigma-Aldrich. Human thrombin was from GE Healthcare. Recombinant human TNF α , FGF-2 and IGF-1 LR3 were from R&D Systems. Blebbistatin and 40 kDa FITC-dextran were from Sigma-Aldrich. Bovine collagen I was from Advanced BioMatrix.

Human plasma fibronectin and bovine gelatin were from Sigma-Aldrich. A rabbit MAB to srGAP2 was from Abcam. A mouse MAB to α -tubulin was from Sigma-Aldrich. A mouse MAB to VE-cadherin was from BD Pharmingen. A rabbit polyclonal antibody to ZO-1 was from Thermo Fisher Scientific. Secondary anti-IgG antibodies conjugated with HRP were from Jackson ImmunoResearch. siRNA oligonucleotides targeting srGAP2 were synthesized by Eurofins Scientific; siRNA1, GUACUACAUCUCCAUCCACCUA; and siRNA2, CCAAUGCAUCUGUCUCCAATT. A universal negative control siRNA oligonucleotide was from Sigma-Aldrich.

Cell culture and transfection

Primary human umbilical vein endothelial cells (HUVEC) from pooled donors (Lonza) were cultured at 37°C in complete endothelial cell growth media (EGM-2) without VEGF (Lonza). For the permeability and the immunofluorescence assays, cells were plated onto surfaces previously coated with 30 μ g/mL of collagen I, 50 μ g/mL fibronectin and 0.1% gelatin. In some experiments, cells were plated onto plastic surfaces previously coated with 5 μ g/mL fibronectin. Cells were used between passages 4 and 6. Cells were transfected with siRNA oligonucleotides using the GeneFECTOR transfection reagent (Venn Nova) according to the manufacturer's protocol and with a 3-h incubation period. Cells were seeded 5 h after transfection and experiments were performed 48 h later. For permeability experiments, ECs were cultured in HIFA2 media 24 h prior to the experiments. This was prepared from EGM-2 as previously described (2). Briefly, EGM-2 was prepared without the provided fetal bovine serum, fibroblast growth factor (FGF)-2, Insulin-like growth factor (IGF)-1, endothelial growth factor or VEGF supplements. This medium was then supplemented with 10 ng/mL recombinant human FGF-2 and 20 ng/mL recombinant IGF-1 LR3.

Western blotting

HUVEC were washed once with PBS and harvested in 2 \times Laemmli buffer (124 mM Tris pH 6.8, 10 mM EDTA pH 6.8, 20% (v/v) glycerol, 4% (w/v) SDS, 200 mM DTT and 0.2% (w/v) bromophenol blue). Proteins were analyzed by SDS-PAGE on 10% (w/v) polyacrylamide gels. Proteins were transferred to polyvinyl fluoride membranes (Merck Millipore) for immunoblotting. The membrane was incubated with ECL reagents (Promega) for 1 min and the signal was detected by exposure to Hyperfilm (GE Healthcare).

Immunofluorescence microscopy

HUVEC were fixed in 4% paraformaldehyde (Thermo Fisher Scientific), permeabilized with 0.2% Triton X-100 (Sigma-Aldrich) and treated with 0.1% sodium borohydride (Sigma-Aldrich). Confocal microscopy was performed using a Leica SP5 AOBS confocal laser-scanning microscope with an attached Leica DM I6000 inverted microscope. Confocal sections were taken through the z-plane and processed to form a 2D projection representing the full depth of the cell culture.

Measuring endothelial permeability

HUVEC (3×10^5 cells/mL) were cultured in Transwell inserts (Sigma-Aldrich) for 48 h until confluent. Then, 1 mg/mL FITC-dextran (40 kDa) and 1 U/mL thrombin were added to the top chamber. Medium was collected at intervals from the lower chamber, and fluorescence was measured in a fluorimeter.

Imaging barrier integrity

HUVEC (3×10^5 cells/mL) were cultured in 24-well plates for 48 h until they formed a monolayer. The plate was introduced into IncuCyte ZOOM Live Cell Analysis System (Sartorius, Goettingen, Germany). An initial image was taken before the addition of permeability factors. Images were taken at 20 \times magnification every 10 min for 6 h. Results were processed and quantified using Image J (12).

RhoA activation assays

HUVEC were cultured in six-well plates for 48 h until they formed a monolayer as previously described. Cells were stimulated with 1 U/mL thrombin across a 90 min time course. Cells were then harvested and processed using the RhoA G-LISA activation assay kit (Cytoskeleton Inc, Denver, CO, USA) according to the manufacturer's protocol.

Statistical analysis

Statistical analysis was performed using GraphPad Prism software. Statistical significance was determined using two-way ANOVA followed by Tukey's *post hoc* test. $*P \leq 0.05$, $**P \leq 0.01$, $***P \leq 0.001$, $****P \leq 0.0001$. All results are reported as mean \pm S.E.M.

Results

srGAP2 limits junctional opening in response to thrombin

Amado-Azevedo and colleagues assessed endothelial barrier opening by measuring the electrical impedance of the endothelial monolayer (11). In that technique, ion conductance across the endothelial layer is used as a surrogate for measuring transport. Impedance measurements allow for assay of rapid changes to paracellular opening but can be affected by other parameters, such as cell morphology (13). We first confirmed the role of srGAP2 in thrombin-mediated permeability by measuring the passage of FITC-dextran. In this well-established *in vitro* assay of endothelial permeability, ECs are grown as a monolayer on permeable Transwell filters. The fluorescent fluid-phase marker FITC-dextran is added to the top chamber and its passage across the endothelial barrier is measured over time by determining the fluorescence of the media in the bottom chamber (13). This technique also has caveats but serves as a useful partner to impedance assays (13). To silence srGAP2 expression, we tested two independent siRNAs and showed that both reduced the expression of srGAP2 in ECs >70% (Fig. 1A). To measure EC permeability, we grew HUVEC to confluence on Transwell filters before moving them into HIFA2 – a serum-free EC medium that we optimized previously for the preservation of HUVEC barrier function (14). In keeping with the findings of Amado-Azevedo *et al.* (11), silencing of srGAP2 led to a significant increase in permeability in response to thrombin treatment. Interestingly, this increase was apparent only at later time points (Fig. 1B). Silencing of srGAP2 had no effect on basal permeability (Fig. 1B).

Amado-Azevedo and colleagues noted that the major effect of srGAP2 depletion was on the recovery of barrier function after thrombin treatment (11), which would be in keeping with the lack of observed effect at early time points in our FITC-dextran assay. Thrombin leads to the opening of junctions between ECs, and recovery is through the re-establishment of those junctions. To visualize junctional dynamics directly, we used an IncuCyte ZOOM Live Cell Analyzer to record live phase-contrast images of the cells across the time course. We wanted an assay that allowed us to focus specifically on the opening and closing of the paracellular space. Treatment with thrombin caused the appearance of visible gaps between cells, which then resolved as barrier function was restored (Fig. 1C). In resting ECs depleted of srGAP2, the size and extent of intracellular gaps were indistinguishable from the control cells (Fig. 1E), and there was no apparent difference in junctional integrity

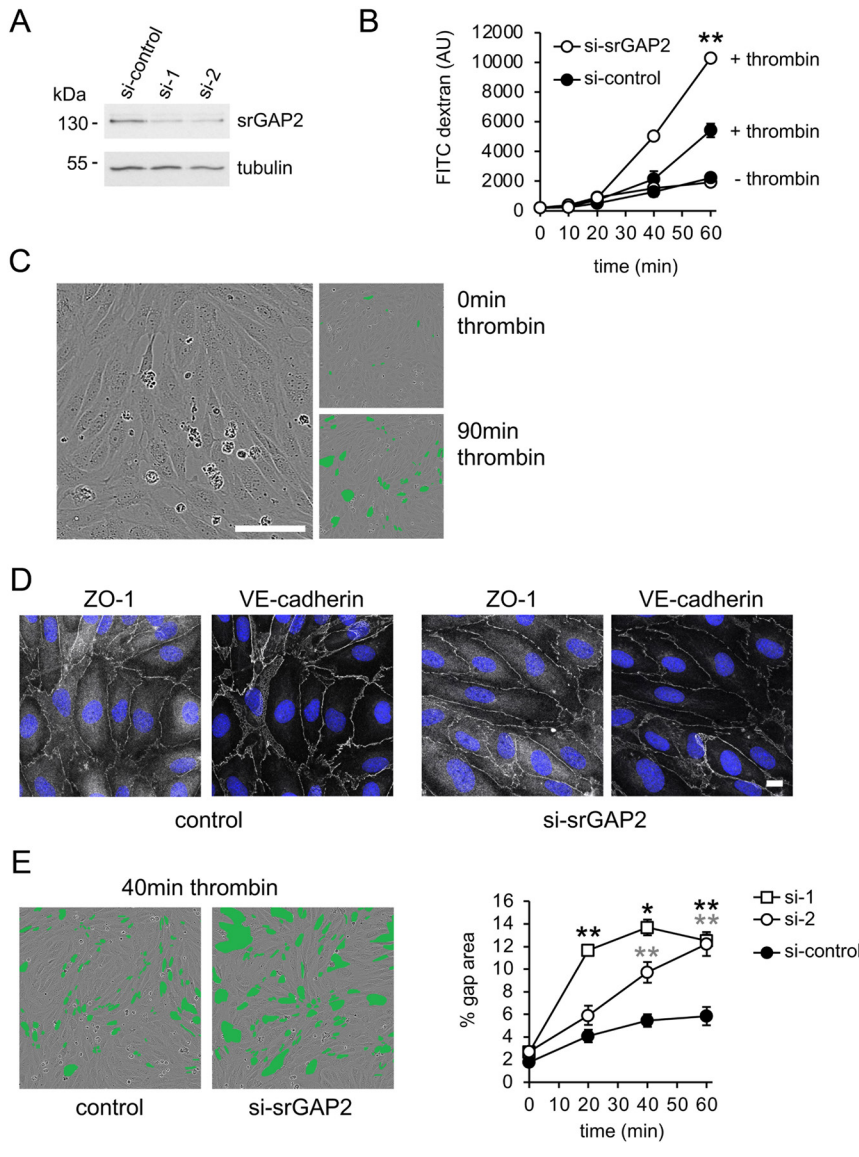


Figure 1 srGAP2 limits junctional opening in response to thrombin. (A) ECs were transfected with two independent srGAP2 siRNAs or a control siRNA and the effectiveness of silencing was determined by western blotting. Each srGAP2 siRNA reduced srGAP2 expression by >70%. (B) ECs were treated ± srGAP2 siRNA and cultured to confluence on Transwell filters. After 48 h, 1 mg/mL FITC-dextran and 1 U/mL thrombin were added to the top chamber. Control cells were treated with vehicle alone. The passage of FITC-dextran across the monolayer was measured by fluorimetry over a 1-h time course. Silencing of srGAP2 increased the permeability after thrombin stimulation but had no effect on resting permeability. Data are means ± s.e.m. (*n* = 3); ***P* ≤ 0.01. (C) ECs were cultured to confluence and brightfield phase images collected using an IncuCyte ZOOM imaging system. The main panel shows a typical starting image. Rounded cells above the monolayer are a mixture of apoptotic and mitotic cells. Cells were stimulated with 1 U/mL thrombin for 90 min. Gaps between cells were manually traced and are highlighted in green here for ease of viewing. Thrombin treatment led to a marked increase in intercellular gaps. Scale bar = 100 μm. (D) ECs were treated ± srGAP2 siRNA and cultured to confluence. After 48 h, cells were fixed and stained for the junctional proteins vascular endothelial cadherin (VE-cadherin) and zonula occludins-1 (ZO-1). Silencing of srGAP2 had no visible effect on junction integrity. Scale bar = 10 μm. (E) ECs were treated ± srGAP2 siRNA and cultured to confluence. After 48 h, cells were stimulated with 1 U/mL thrombin across a 90 min time course. The panels show representative images obtained at 40 min post-stimulation. Quantification of the image data showed that silencing of srGAP2 significantly increased the number and size of intercellular gaps after thrombin stimulation. Data are means ± s.e.m. (*n* = 6). ***P* ≤ 0.01; **P* ≤ 0.05 (si-1; black asterisks, si-2; gray asterisks).

as assessed by staining for vascular endothelial cadherin (VE-cadherin) and ZO-1 (Fig. 1D). However, the initial rate and extent of the junctional opening were far greater on thrombin treatment and junctions did not reform properly within 90 min (Fig. 1E). We conclude that srGAP2 acts to limit junctional opening in response to thrombin.

srGAP2 limits junctional opening in response to TNFα and angiotensin II

To determine whether srGAP2 acts specifically on thrombin-induced permeability, we examined two alternative regulators of endothelial barrier function. TNFα is a pro-inflammatory chemokine that drives endothelial permeability during sepsis (15, 16). Ang II is

a potent vasoconstrictor and regulator of blood pressure, but also increases vascular permeability (17). Both factors act to increase leukocyte infiltration of tissue during inflammation. TNFα treatment led to slower junction opening in ECs than thrombin and junctions remained open for far longer (Fig. 2A). Depletion of srGAP2 had no effect on the initial rate of junction opening but led to a significant increase in transcellular gaps at later time points (Fig. 2A). In ECs treated with Ang II, depletion of srGAP2 increased junction opening at early time points, and also significantly inhibited the closing of junctions in the recovery phase (Fig. 2B).

We conclude that srGAP2 restricts the degree of endothelial barrier opening in response to three very different mediators of vascular permeability. srGAP2

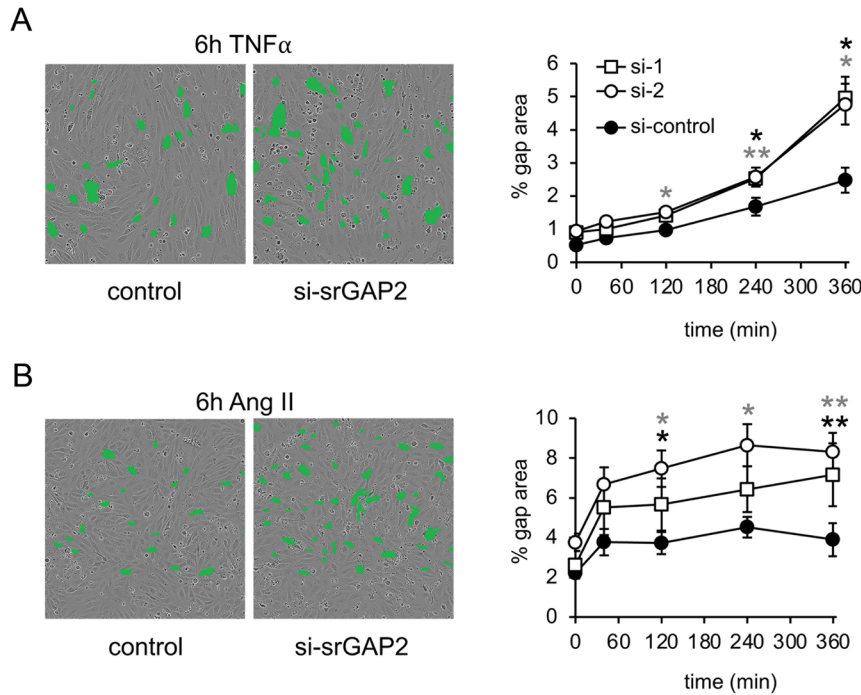


Figure 2
srGAP2 limits junctional opening in response to TNF α and angiotensin II. (A) ECs were treated \pm srGAP2 siRNA and cultured to confluence. After 48 h, cells were stimulated with 10 ng/mL TNF- α over a 6-h time course. The panels show representative images obtained 6-h post-stimulation. Quantification of the image data showed that silencing of srGAP2 significantly increased the number and size of intercellular gaps after TNF- α stimulation. Data are means \pm s.e.m. ($n = 5$). ** $P \leq 0.01$; * $P \leq 0.05$ (si-1; black asterisks, si-2; gray asterisks). (B) ECs were treated \pm srGAP2 siRNA and cultured to confluence. After 48 h, cells were stimulated with 10 μ M Ang II over a 6-h time course. The panels show representative images obtained 6-h post-stimulation. Quantification of the image data showed that silencing of srGAP2 significantly increased the number and size of intercellular gaps after Ang II stimulation. Data are means \pm s.e.m. ($n = 5$). * $P \leq 0.05$ (si-1; black asterisk, si-2; gray asterisk).

dampens junctional opening in response to thrombin and Ang II, but not to TNF α . The length of the junctional opening varies between the three mediators, but in all three cases, srGAP2 is required for effective reclosure of junctions after exposure to the permeability trigger.

srGAP2 delays the respreading of endothelial cells after thrombin-mediated junction opening

The opening of endothelial junctions involves destabilization of interactions between cell-cell adhesion proteins coupled with the generation of a contractile force (7, 18). The subsequent reclosing of junctions requires respreading of ECs along the vascular wall (a protrusive movement), followed by stabilization of cell-cell adhesions. In our assay, the initial rate of intracellular gap formation is a combination of the time taken to breakdown junctions and the rate of cell retraction. In order to separate the rates of contraction and respreading from the rate of junction breakdown, we plated ECs sparsely and then treated them with thrombin as before. Cells were then free to contract in response to thrombin without needing to first disassemble junctions. We measured cell area over time to derive the rates of contraction and respreading. Depletion of srGAP2 had no effect on the rate of EC retraction in response to thrombin; however, it significantly delayed the rate of respreading (Fig. 3A).

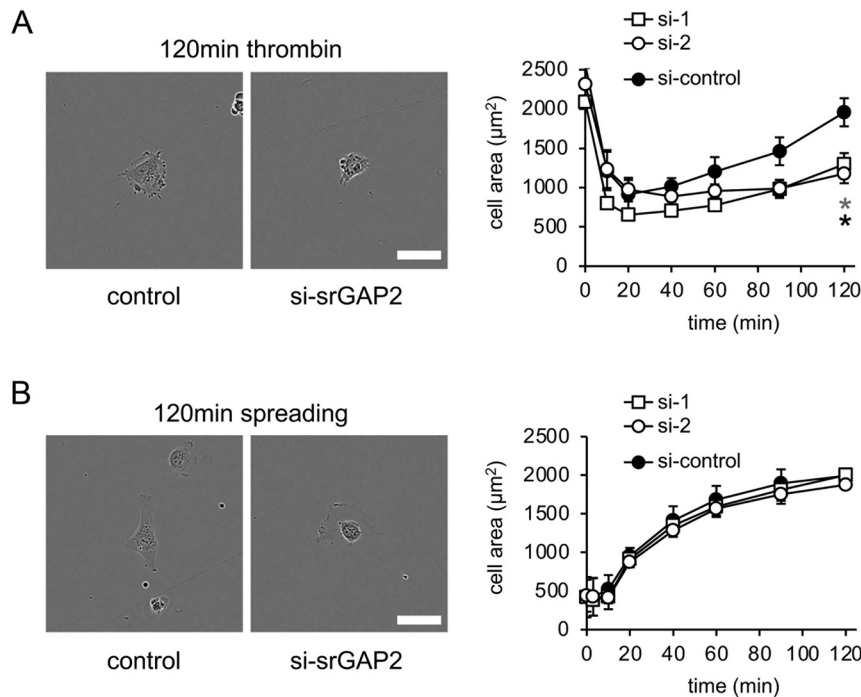
These results raised the possibility that srGAP2 may simply be required for the mechanical processes of cell

spreading. To examine this, we detached ECs by gentle trypsinization and then allowed them to settle and spread while imaging their surface areas. Intriguingly, the deletion of srGAP2 had no effect on the ability of unstimulated ECs to spread (Fig. 3B). We conclude that srGAP2 is required for efficient respreading of ECs after thrombin-driven retraction.

srGAP2 controls the duration of RhoA activation in response to thrombin

Thrombin, TNF α and Ang II all signal through different EC receptors to trigger vascular permeability. Thrombin acts via the PAR1 receptor, TNF α via TNF receptor 1 and Ang II through the AT1 receptor (19, 20, 21). Further, these three permeability mediators appear to act in multiple ways to increase permeability. One thing that all three have in common is the activation of the small GTPase RhoA, which is the major regulator of cellular contraction (22). Activation of RhoA leads to the generation of the contractile force involved in the opening of EC junctions and re-establishment of barrier function requires turning off the RhoA signal (8). srGAP2 is part of a large family of Rho GAP proteins that catalyze the inactivation of Rho GTPases and return them to their inactive state (10). We therefore examined whether srGAP2 was regulating RhoA activation kinetics in ECs in response to thrombin.

Stimulation of ECs with thrombin gave a six-fold increase in RhoA activity that peaked at 10 min and slowly

**Figure 3**

srGAP2 delays the respreading of endothelial cells after thrombin-mediated junction opening. (A) ECs were treated \pm srGAP2 siRNA and plated at low density. After 48 h, cells were stimulated with 1 U/mL thrombin over a 2-h time course. The panels show representative images obtained 2-h post-stimulation. Quantification of the image data showed that silencing of srGAP2 had no effect on the initial retraction phase, but significantly reduced respreading. Data are means \pm s.e.m. ($n = 4$). $**P \leq 0.01$; $*P \leq 0.05$ (si-1; black asterisks, si-2; gray asterisks). (B) ECs were treated \pm srGAP2 siRNA and plated at low density without thrombin treatment and allowed to spread normally over a 2-h time course. The panels show representative images obtained 2 h after plating. Quantification of the image data showed that silencing of srGAP2 had no effect on the adhesion or spreading of untreated ECs. Data are means \pm s.e.m. ($n = 4$). Scale bars = 50 μm .

declined as the cells respread. Depletion of srGAP2 caused an increase in the peak activation of RhoA; however, the major effect was on the deactivation phase, which was significantly slower in cells lacking srGAP2, where active RhoA levels remained elevated (Fig. 4A). Resting levels of RhoA activity were unaffected by depletion of srGAP2, in accordance with the lack of effect on resting permeability. We conclude that srGAP2 acts to control the duration of RhoA signaling in thrombin-mediated permeability.

The protective effects of srGAP2 are mimicked by inhibition of actinomyosin contraction

Activation of the RhoA pathway in ECs triggers cell contraction by promoting increased actinomyosin contractility (8). RhoA signaling leads to activation of myosin II motor activity through increased phosphorylation of the myosin light chain (6, 7). This increased actinomyosin contractility can be reversed by treatment with blebbistatin, a cell-permeant myosin II inhibitor (23). We treated ECs with thrombin for 40 min and then measured the effect of blebbistatin on the paracellular gap area. Treatment of control ECs with blebbistatin caused a small decrease in the area of open gaps after thrombin treatment (Fig. 4B). However, blebbistatin had a major effect on gap opening in srGAP2 depleted cells and was able to almost fully restore cells to the normal response (Fig. 4B).

We conclude that srGAP2 promotes recovery of barrier function after thrombin treatment by promoting deactivation of RhoA and actinomyosin contractility to promote the switch to EC respreading (Fig. 5).

Discussion

The regulated opening and closing of endothelial cell junctions are key components of the physiological function of the endothelium. During sepsis, retraction of ECs can lead to dysregulated thrombosis and organ failure (24, 25). Theoretically, drug targeting of RhoA would reduce EC contraction and help restore barrier function. However, RhoA is a central node in cytoskeletal signaling (22) and inhibition of RhoA activity would be expected to be highly toxic. Indeed, several bacterial toxins exhibit their toxicity by targeting RhoA activity (26). The Rho GTPase GEFs and GAPs are large families of multi-domain proteins that give specificity to Rho GTPase signaling by linking Rho GTPase dynamics to specific signals (9, 10). Targeting of specific Rho GEFs or GAPs then represents a potential strategy for the selective blockage of specific Rho pathways in specific cellular contexts (27).

The recent study by Amado-Azevedo and colleagues is an important contribution to our understanding of Rho GTPases signaling in endothelial permeability. Their screen of 270 Rho-associated genes allowed identification

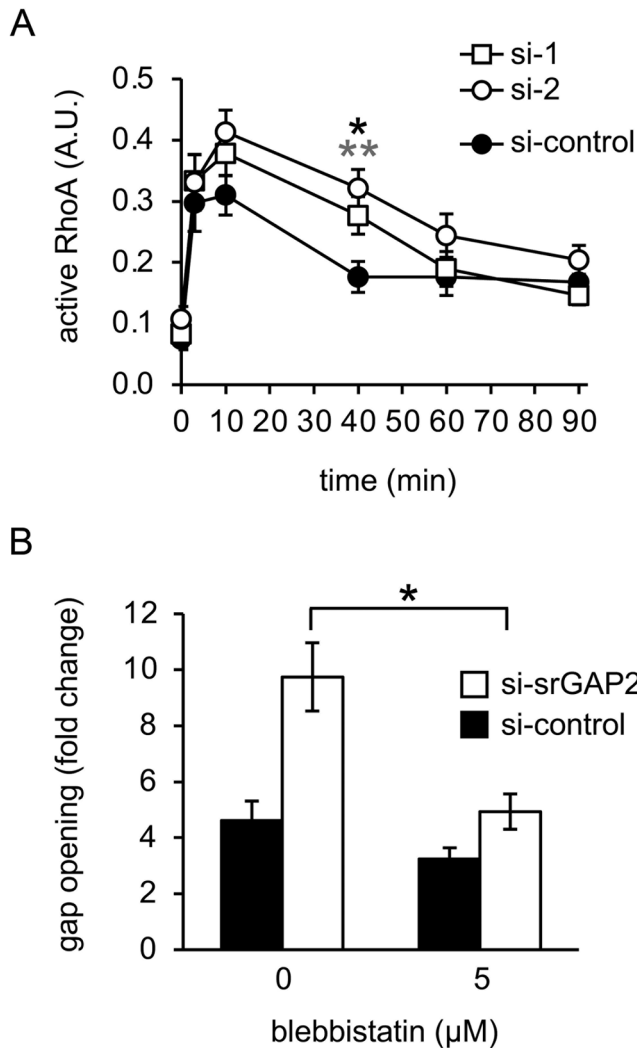


Figure 4 srGAP2 controls the duration of RhoA activation in response to thrombin. (A) ECs were treated ± srGAP2 siRNA and cultured to confluence. After 48 h, cells were stimulated with 1 U/mL thrombin over a 90 min time course. At each time point, cells were lysed and active RhoA levels were measured by G-LISA. Silencing of srGAP2 led to increased RhoA activation after thrombin stimulation and RhoA deactivation was significantly delayed. Data are means ± s.e.m. (*n* = 9). ***P* ≤ 0.01; **P* ≤ 0.05 (si-1; black asterisks, si-2; gray asterisks). (B) HUVEC were treated ± srGAP2 siRNA and cultured to confluence. After 48 h, cells were incubated with 5 μM blebbistatin or vehicle for 1 h. Cells were then stimulated with 1 U/mL thrombin for 40 min. The fold-increase in gap area was calculated in comparison to untreated control cells. Blebbistatin slightly reduced gap formation in control cells. In ECs depleted of srGAP2, blebbistatin returned thrombin-induced gap formation to near normal levels. Data are means ± s.e.m. (*n* = 7). **P* ≤ 0.05.

of the key Rho GTPase regulators in this important process. The study identified four Rho family GEFs; the proteins that regulate Rho GTPase activation (11). Interestingly, three of them (TIAM2/STEF, PREX1 and ARHGEF7/β-PIX) are activators of Rac1, which is required for respreading

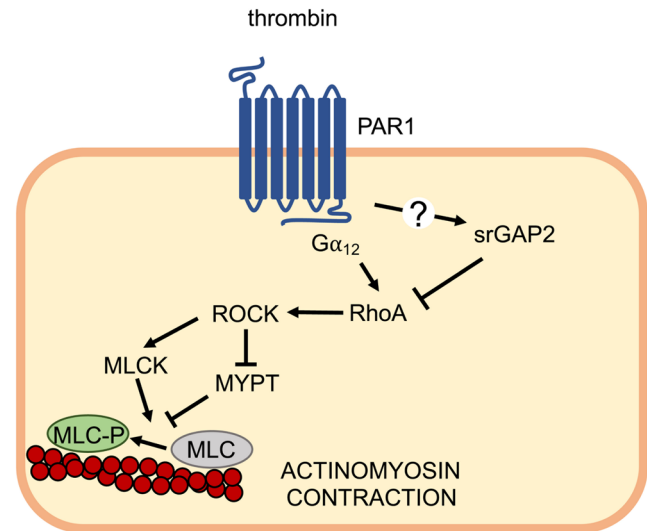


Figure 5 A model for srGAP2 action in thrombin-mediated vascular permeability. Binding of thrombin to the PAR1 receptor leads to activation of the small GTPase Gα₁₂, which then triggers activation of RhoA via GEF activation. RhoA drives phosphorylation of MLC to increase the force of actinomyosin contraction, which then leads to retraction of the cell. In the model, srGAP2 controls the inactivation of this thrombin-induced RhoA signal, limiting the extent of gap opening and allowing the respreading phase where junctions can be reformed. It is unclear whether PAR1 signaling leads to activation of srGAP2, or whether srGAP2 is a constitutively active factor in this pathway.

and reformation of cell-cell junctions after barrier opening. Each is involved in different cellular locations of Rac action, underscoring how GEFs provide important spatial and temporal regulation to Rho GTPase signaling. ARHGEF5/TIM was identified as the key RhoA GEF in thrombin-induced permeability, with possible smaller contributions by LARG and GEF-H1 (11). Importantly, recent studies have shown that TIM can be both activated (28) and inhibited (29) by peptide-based drugs to control its activity in cells, raising the possibility of clinical manipulation of thrombin-induced RhoA signaling pathways downstream of this GEF.

The same study identified three Rho GAPs as regulators of thrombin-induced permeability – ARHGAP45/HMHA1, RacGAP1/MgcRacGAP and srGAP2. HMHA1 is a Rac GAP, and the same researchers subsequently confirmed that it acts to reduce Rac1 activity in ECs, leading to reduced barrier function in resting cells (30). RacGAP1 is also a Rac GAP (31), although it has been shown to change specificity on phosphorylation to become a RhoA GAP (32). Initial studies showed that purified srGAP2 also inactivates Rac1, with much lower activity against RhoA and Cdc42 (33, 34). More recent work has shown that srGAP2 acts on RhoA and Cdc42 in podocytes and not Rac1 (35). It is clear that GAP

specificity *in vivo* can be context dependent and, as RacGAP1 shows, specificity can be switched through regulation. The effects of silencing srGAP2 on EC barrier functions did not tally with expectations of a Rac GAP, but rather the delayed respreading of cells suggested a link to RhoA. Indeed, measurement of RhoA activity in srGAP2 depleted ECs allowed us to show that srGAP2 was acting as a RhoA GAP in the context of thrombin-mediated permeability and so to explain enhanced retraction observed on the loss of srGAP2 function. The mechanisms controlling srGAP2 specificity switching require further investigation and may also be useful in the potential clinical manipulation of srGAP2 function.

Silencing of srGAP2 led to increased RhoA activation and a slower inactivation rate (Fig. 4A). Previous studies have shown that the p190RhoGAP can regulate EC junctional stability through the inactivation of RhoA (18). Interestingly, p190RhoGAP is localized to EC junction by p120 catenin, localizing its actions to that site (35). It has been shown that p190RhoGAP is required for the stabilization of EC junctions caused by angiopoietin-1 (36) and that nitric oxide production leads to inactivation of p190GAP via nitrosylation, leading to destabilization of junctions and increased permeability (37). As silencing of srGAP2 did not completely block RhoA inactivation, it is possible that other Rho GAPs may also be involved; however, Amado-Azevedo and colleagues found no role for p190GAP in thrombin-mediated permeability (11). It is still possible that other Rho GAPs may play a part in this; however, it is also possible that the intrinsic rate of GTP hydrolysis of RhoA is responsible for the eventual inactivation in cells depleted of srGAP2.

Our model for srGAP2 function in thrombin-mediated permeability highlights a missing component – the upstream regulator of srGAP2 in the pathway (Fig. 5). The regulation of srGAP2 is currently poorly understood. The related protein srGAP1 was named for its direct interaction with the Robo1 receptor. In neurons, activation of the Robo1 receptor by the guidance cue Slit leads to repulsive signals that involve regulation of Cdc42 activity by srGAP1 (38). We were unable to detect any interaction between srGAP2 and the thrombin receptor (data not shown), however, suggesting that srGAP2 must be regulated in a different way. The srGAP proteins all contain an N-terminal F-BAR domain. This domain allows proteins to sense membrane curvature and srGAP proteins are recruited to regions of positive membrane curvature (i.e. outward deformation; (39)). In migrating fibroblasts, srGAP2 has been shown to be recruited to areas of membrane protrusion at the leading edge of those cells (40). This raises the intriguing

possibility that srGAP2 can ‘read’ the membrane geometry during a cycle of junction opening and reclosing. In this model, srGAP2 would be recruited to the protrusive edge of the retracted EC as it begins to respread, consolidating the protrusive phase. Such a model would explain why srGAP2 can act generally on the three specific permeability pathways that we examined.

srGAP2 is highly conserved across vertebrates (18). Previous work has shown that it is highly expressed in the brain during development, where it regulates neuronal migration (33). Importantly, the srGAP2 gene underwent two partial gene duplication events during human evolution to produce two truncation gene products; srGAP2B and srGAP2C ((41); the parental gene is referred to as srGAP2A in humans). srGAP2C acts as a cellular inhibitor of srGAP2A, limiting its action in neurons and allowing increased synaptic density during brain development (42). These paralogs of srGAP2 are important for being two of the handful of genes that are unique to our species. Recent work has provided evidence that the gain of srGAP2C contributed to the unique development of the human brain, altering srGAP2A signaling to allow human-specific adaptations of neural development (42, 43, 44). The other human-specific genes similarly define specific and important differences between our species and other animals. srGAP2C would be expected to limit srGAP2A activity and so promote paracellular permeability in response to inflammatory mediators. This raises the intriguing possibility that the regulation of vascular permeability in humans may be adapted compared to other mammals. It will be important to examine these potential differences in detail – and especially for species that are commonly used as models in studies of endothelial permeability.

Declaration of interest

The authors declare that there is no conflict of interest that could be perceived as prejudicing the impartiality of the research reported.

Funding

This work was supported by the British Heart Foundation (grant number FS/17/42/32978).

Author contribution statement

Conceptualization, H M; Methodology, A R L, A F and H M; Investigation, A R L and A F; Writing – Original Draft, H M; Writing – Review and Editing, A R L; Funding Acquisition, H M; Resources, H M, Supervision, H M.

Acknowledgement

The authors would like to thank Sophie Bacon for contributions to the pilot work on this study.

References

- Galley HF & Webster NR. Physiology of the endothelium. *British Journal of Anaesthesia* 2004 **93** 105–113. (<https://doi.org/10.1093/bja/aeh163>)
- Komarova Y & Malik AB. Regulation of endothelial permeability via paracellular and transcellular transport pathways. *Annual Review of Physiology* 2010 **72** 463–493. (<https://doi.org/10.1146/annurev-physiol-021909-135833>)
- Yazdani S, Jaldin-Fincati JR, Pereira RVS & Klip A. Endothelial cell barriers: transport of molecules between blood and tissues. *Traffic* 2019 **20** 390–403. (<https://doi.org/10.1111/tra.12645>)
- Dejana E. Endothelial cell-cell junctions: happy together. *Nature Reviews: Molecular Cell Biology* 2004 **5** 261–270. (<https://doi.org/10.1038/nrm1357>)
- Claesson-Welsh L. Vascular permeability – the essentials. *Upsala Journal of Medical Sciences* 2015 **120** 135–143. (<https://doi.org/10.3109/03009734.2015.1064501>)
- Cerutti C & Ridley AJ. Endothelial cell-cell adhesion and signaling. *Experimental Cell Research* 2017 **358** 31–38. (<https://doi.org/10.1016/j.yexcr.2017.06.003>)
- Belvitch P, Htwe YM, Brown ME & Dudek S. Cortical actin dynamics in endothelial permeability. *Current Topics in Membranes* 2018 **82** 141–195. (<https://doi.org/10.1016/bs.ctm.2018.09.003>)
- Wojciak-Stothard B & Ridley AJ. Rho GTPases and the regulation of endothelial permeability. *Vascular Pharmacology* 2002 **39** 187–199. ([https://doi.org/10.1016/s1537-1891\(03\)00008-9](https://doi.org/10.1016/s1537-1891(03)00008-9))
- Cook DR, Rossman KL & Der CJ. Rho guanine nucleotide exchange factors: regulators of Rho GTPase activity in development and disease. *Oncogene* 2014 **33** 4021–4035. (<https://doi.org/10.1038/onc.2013.362>)
- Tcherkezian J & Lamarche-Vane N. Current knowledge of the large RhoGAP family of proteins. *Biology of the Cell* 2007 **99** 67–86. (<https://doi.org/10.1042/BC20060086>)
- Amado-Azevedo J, de Menezes RX, van Nieuw Amerongen GP, van Hinsbergh VWM & Hordijk PL. A functional siRNA screen identifies RhoGTPase-associated genes involved in thrombin-induced endothelial permeability. *PLoS ONE* 2018 **13** e0201231. (<https://doi.org/10.1371/journal.pone.0201231>)
- Schneider CA, Rasband WS & Eliceiri KW. NIH Image to ImageJ: 25 years of image analysis. *Nature Methods* 2012 **9** 671–675. (<https://doi.org/10.1038/nmeth.2089>)
- Bischoff I, Hornburger MC, Mayer BA, Beyerle A, Wegener J & Fürst R. Pitfalls in assessing microvascular endothelial barrier function: impedance-based devices versus the classic macromolecular tracer assay. *Scientific Reports* 2016 **6** 23671. (<https://doi.org/10.1038/srep23671>)
- Wei H, Sundaraman A, Dickson E, Rennie-Campbell L, Cross E, Heesom KJ & Mellor H. Characterization of the polarized endothelial secretome. *FASEB Journal* 2019 **33** 12277–12287. (<https://doi.org/10.1096/fj.201900262R>)
- Brett J, Gerlach H, Nawroth P, Steinberg S, Godman G & Stern D. Tumor necrosis factor/cachectin increases permeability of endothelial cell monolayers by a mechanism involving regulatory G proteins. *Journal of Experimental Medicine* 1989 **169** 1977–1991. (<https://doi.org/10.1084/jem.169.6.1977>)
- Goldblum SE & Sun WL. Tumor necrosis factor-alpha augments pulmonary arterial transendothelial albumin flux in vitro. *American Journal of Physiology* 1990 **258** L57–L67. (<https://doi.org/10.1152/ajplung.1990.258.2.L57>)
- Suzuki Y, Ruiz-Ortega M, Lorenzo O, Ruperez M, Esteban V & Egido J. Inflammation and angiotensin II. *International Journal of Biochemistry and Cell Biology* 2003 **35** 881–900. ([https://doi.org/10.1016/s1357-2725\(02\)00271-6](https://doi.org/10.1016/s1357-2725(02)00271-6))
- Radeva MY & Waschke J. Mind the gap: mechanisms regulating the endothelial barrier. *Acta Physiologica* 2018 **222** e12860. (<https://doi.org/10.1111/apha.12860>)
- Ferrero E, Zocchi MR, Magni E, Panzeri MC, Curnis F, Rugarli C, Ferrero ME & Corti A. Roles of tumor necrosis factor p55 and p75 receptors in TNF-alpha-induced vascular permeability. *American Journal of Physiology: Cell Physiology* 2001 **281** C1173–C1179. (<https://doi.org/10.1152/ajpcell.2001.281.4.C1173>)
- Fleegal-DeMotta MA, Doghu S & Banks WA. Angiotensin II modulates BBB permeability via activation of the AT(1) receptor in brain endothelial cells. *Journal of Cerebral Blood Flow and Metabolism* 2009 **29** 640–647. (<https://doi.org/10.1038/jcbfm.2008.158>)
- Vogel SM, Gao X, Mehta D, Ye RD, John TA, Andrade-Gordon P, Tiruppathi C & Malik AB. Abrogation of thrombin-induced increase in pulmonary microvascular permeability in PAR-1 knockout mice. *Physiological Genomics* 2000 **4** 137–145. (<https://doi.org/10.1152/physiolgenomics.2000.4.2.137>)
- Ridley AJ. Rho GTPases and actin dynamics in membrane protrusions and vesicle trafficking. *Trends in Cell Biology* 2006 **16** 522–529. (<https://doi.org/10.1016/j.tcb.2006.08.006>)
- Straight AF, Cheung A, Limouze J, Chen I, Westwood NJ, Sellers JR & Mitchison TJ. Dissecting temporal and spatial control of cytokinesis with a myosin II inhibitor. *Science* 2003 **299** 1743–1747. (<https://doi.org/10.1126/science.1081412>)
- Joffre J, Hellman J, Ince C & Ait-Oufella H. Endothelial responses in sepsis. *American Journal of Respiratory and Critical Care Medicine* 2020 **202** 361–370. (<https://doi.org/10.1164/rccm.201910-1911TR>)
- Ince C, Mayeux PR, Nguyen T, Gomez H, Kellum JA, Ospina-Tascón GA, Hernandez G, Murray P, De Backer D & ADQI XIV Workgroup. The endothelium in sepsis. *Shock* 2016 **45** 259–270. (<https://doi.org/10.1097/SHK.0000000000000473>)
- Aktories K, Schmidt G & Just I. Rho GTPases as targets of bacterial protein toxins. *Biological Chemistry* 2000 **381** 421–426. (<https://doi.org/10.1515/BC.2000.054>)
- Gray JL, von Delft F & Brennan PE. Targeting the small GTPase superfamily through their regulatory proteins. *Angewandte Chemie* 2020 **59** 6342–6366. (<https://doi.org/10.1002/anie.201900585>)
- He P, Tan DL, Liu HX, Lv FL & Wu W. The auto-inhibitory state of Rho guanine nucleotide exchange factor ARHGEF5/TIM can be relieved by targeting its SH3 domain with rationally designed peptide aptamers. *Biochimie* 2015 **111** 10–18. (<https://doi.org/10.1016/j.biochi.2015.01.011>)
- Huang O, Wu D, Xie F, Lin L, Wang X, Jiang M, Li Y, Chen W, Shen K & Hu X. Targeting rho guanine nucleotide exchange factor ARHGEF5/TIM with auto-inhibitory peptides in human breast cancer. *Amino Acids* 2015 **47** 1239–1246. (<https://doi.org/10.1007/s00726-015-1950-0>)
- Amado-Azevedo J, Reinhard NR, van Bezu J, van Nieuw Amerongen GP, van Hinsbergh VWM & Hordijk PL. The minor histocompatibility antigen 1 (HMHA1)/ArhGAP45 is a RacGAP and a novel regulator of endothelial integrity. *Vascular Pharmacology* 2018 **101** 38–47. (<https://doi.org/10.1016/j.vph.2017.11.007>)
- Bastos RN, Penate X, Bates M, Hammond D & Barr FA. CYK4 inhibits Rac1-dependent PAK1 and ARHGEF7 effector pathways during cytokinesis. *Journal of Cell Biology* 2012 **198** 865–880. (<https://doi.org/10.1083/jcb.201204107>)
- Minoshima Y, Kawashima T, Hirose K, Tonozuka Y, Kawajiri A, Bao YC, Deng X, Tatsuka M, Narumiya S, May WS, *et al.* Phosphorylation by aurora B converts MgcRacGAP to a RhoGAP during cytokinesis. *Developmental Cell* 2003 **4** 549–560. ([https://doi.org/10.1016/s1534-5807\(03\)00089-3](https://doi.org/10.1016/s1534-5807(03)00089-3))
- Guerrier S, Coutinho-Budd J, Sassa T, Gresset A, Jordan NV, Chen K, Jin WL, Frost A & Polleux F. The F-BAR domain of srGAP2 induces

- membrane protrusions required for neuronal migration and morphogenesis. *Cell* 2009 **138** 990–1004. (<https://doi.org/10.1016/j.cell.2009.06.047>)
- 34 Mason FM, Heimsath EG, Higgs HN & Soderling SH. Bi-modal regulation of a formin by srGAP2. *Journal of Biological Chemistry* 2011 **286** 6577–6586. (<https://doi.org/10.1074/jbc.M110.190397>)
- 35 Zebda N, Tian Y, Tian X, Gawlak G, Higginbotham K, Reynolds AB, Birukova AA & Birukov KG. Interaction of p190RhoGAP with C-terminal domain of p120-catenin modulates endothelial cytoskeleton and permeability. *Journal of Biological Chemistry* 2013 **288** 18290–18299. (<https://doi.org/10.1074/jbc.M112.432757>)
- 36 Mammoto T, Parikh SM, Mammoto A, Gallagher D, Chan B, Mostoslavsky G, Ingber DE & Sukhatme VP. Angiopoietin-1 requires p190 RhoGAP to protect against vascular leakage in vivo. *Journal of Biological Chemistry* 2007 **282** 23910–23918. (<https://doi.org/10.1074/jbc.M702169200>)
- 37 Siddiqui MR, Komarova YA, Vogel SM, Gao X, Bonini MG, Rajasingh J, Zhao YY, Brovkovych V & Malik AB. Caveolin-1-eNOS signaling promotes p190RhoGAP-A nitration and endothelial permeability. *Journal of Cell Biology* 2011 **193** 841–850. (<https://doi.org/10.1083/jcb.201012129>)
- 38 Wong K, Ren XR, Huang YZ, Xie Y, Liu G, Saito H, Tang H, Wen L, Brady-Kalnay SM, Mei L, *et al.* Signal transduction in neuronal migration: roles of GTPase activating proteins and the small GTPase Cdc42 in the Slit-Robo pathway. *Cell* 2001 **107** 209–221. ([https://doi.org/10.1016/S0092-8674\(01\)00530-X](https://doi.org/10.1016/S0092-8674(01)00530-X))
- 39 Lucas B & Hardin J. Mind the (sr)GAP – roles of slit-Robo GAPs in neurons, brains and beyond. *Journal of Cell Science* 2017 **130** 3965–3974. (<https://doi.org/10.1242/jcs.207456>)
- 40 Fritz RD, Menshykau D, Martin K, Reimann A, Pontelli V & Pertz O. SrGAP2-dependent integration of membrane geometry and slit-Robo-repulsive cues regulates fibroblast contact inhibition of locomotion. *Developmental Cell* 2015 **35** 78–92. (<https://doi.org/10.1016/j.devcel.2015.09.002>)
- 41 Dennis MY, Nuttle X, Sudmant PH, Antonacci F, Graves TA, Nefedov M, Rosenfeld JA, Sajjadian S, Malig M, Kotkiewicz H, *et al.* Evolution of human-specific neural SRGAP2 genes by incomplete segmental duplication. *Cell* 2012 **149** 912–922. (<https://doi.org/10.1016/j.cell.2012.03.033>)
- 42 Charrier C, Joshi K, Coutinho-Budd J, Kim JE, Lambert N, de Marchena J, Jin WL, Vanderhaeghen P, Ghosh A, Sassa T, *et al.* Inhibition of SRGAP2 function by its human-specific paralogs induces neoteny during spine maturation. *Cell* 2012 **149** 923–935. (<https://doi.org/10.1016/j.cell.2012.03.034>)
- 43 Schmidt ERE, Kupferman JV, Stackmann M & Polleux F. The human-specific paralogs SRGAP2B and SRGAP2C differentially modulate SRGAP2A-dependent synaptic development. *Scientific Reports* 2019 **9** 18692.
- 44 Fossati M, Pizzarelli R, Schmidt ER, Kupferman JV, Stroebel D, Polleux F & Charrier C. SRGAP2 and its human-specific paralog co-regulate the development of excitatory and inhibitory synapses. *Neuron* 2016 **91** 356–369. (<https://doi.org/10.1016/j.neuron.2016.06.013>)

Received in final form 12 February 2022

Accepted 28 February 2022

Accepted Preprint published online 28 February 2022